Interspike interval statistics of a leaky integrate-and-fire neuron driven by Gaussian noise with large correlation times

Tilo Schwalger[1,2] and Lutz Schimansky-Geier[1]
[1]*Humboldt-Universität Berlin, Newtonstrasse 15, D-12489 Berlin, Germany*
[2]*RIKEN Brain Science Institute, 2-1 Hirosawa, Wako, Saitama 351-0198, Japan*
(Received 25 October 2007; revised manuscript received 19 December 2007; published 14 March 2008)

We analytically investigate the interspike interval (ISI) density, the Fano factor, and the coefficient of variation of a leaky integrate-and-fire neuron model driven by exponentially correlated Gaussian noise with a large correlation time τ. We find a burstinglike behavior of the spike train, which is revealed by a dominant peak of the ISI density at small intraburst intervals and a slow power-law decay of long interburst intervals. The large, power-law distributed ISIs give rise to a coefficient of variation which diverges as $\sqrt{\tau}$. This leads to the paradoxical effect that ISI correlations, as expressed by the serial correlation coefficient, vanish for large correlation times. This is in contrast to findings of previous works on a simpler neuron model where the effect of noise correlations appeared in higher-order statistical measures.

DOI: 10.1103/PhysRevE.77.031914 PACS number(s): 87.19.L−, 05.40.Ca

I. INTRODUCTION

Understanding the dynamics and information processing of neurons as the basic units of the gigantic cortical network is of fundamental interest. Thereby researchers face the problem of the exceedingly complex dynamics of neurons in this network. For instance, already a single neuron undergoes a permanent input of spikes from thousands of other neurons, leading to stochastic excitation of the neuron and spike emission. To capture such complexity in a mathematically accessible model, the incoming spike trains are often assumed to be independent Poisson processes that evoke a large number of tiny postsynaptic potentials. Under the assumption of negligible small synaptic time constants this allows one to approximate the total synaptic input to the neuron by a mean current added with Gaussian white noise [1–6]. For those diffusion models there exist well-established tools for an analytical treatment of the associated first-passage-time problem (Fokker-Planck equation, renewal equation).

It is clear, however, that phenomena like synchronous spiking of presynaptic neurons may produce a rich *temporal structure* in the input signal [7]. Neuron models that are driven by only white noise cannot account for such temporal structure, because of the absence of correlations. As a simple extension, colored noise with a correlation time τ could thus be used to study the impact of temporal structure. Note that the related case of periodic driving in the presence of noise, as known in problems of stochastic resonance [8–13], yields an input structure with an infinitely large correlation time. Another source of temporal correlations results from the filtering dynamics at the synapses. Depending on the type of receptor and the state of the neuron, there is a wide range of correlation times that are induced by synaptic filtering [14]. In this paper we attempt to investigate the possible influence of *long-range* correlations in the synaptic input on the statistics of the neurons' output spike train. In contrast to the white noise case, this problem involves the analysis of a process that possesses a strong non-Markovian character.

It should be noted that by now there are several works which addressed this problem. A detailed analysis of the impact of different forms of correlated noise was achieved using the perfect integrate-and-fire (PIF) model [15–17]. This rather simple neuron model integrates the input current without leakage until the neuron's membrane potential hits a threshold, whereupon it is reset to a prefixed value. In such models spikes are implicitly given by the moments of threshold crossing. It has been found that the coefficient of variation (CV), which reflects the variability of the interspike intervals (ISIs), can be significantly increased by colored noise [15]. Furthermore, the ISI density exhibits a power-law decay with exponent −3 in the limit of infinitely large correlation times [16]. The most interesting feature, however, is the finding that the effect of a correlated input appears in the higher-order statistics rather than in the statistics of the single ISI: The spike train, e.g., is most regular on a certain finite time scale as expressed by the Fano factor of the spike count. Moreover, the ISIs become strongly correlated when the correlation time is increased [16,17]. The characteristic, exponential decay of the serial correlation coefficient (SCC) with respect to the lag between ISIs directly translates into the correlation time—"information" that is not given by the ISI density.

The statistics of a renewal process, i.e., a spike train with statistically independent ISIs, is completely described by the ISI density. But it is not clear whether in general a nonrenewal process is best characterized by the ISI density or by higher-order measures. In this work we intend to analyze the more realistic but still simple leaky integrate-and-fire (LIF) neuron model [18]. Due to the inclusion of a leak current the electrical properties of the membrane are described more accurately, which renders the LIF model extremely useful in theoretical studies and network simulations.

Although quite similar to the PIF model, it will turn out that the effect of long-correlated noise is utterly different. There exist some works on colored noise-driven LIF neurons [7,14,15,19–23]. For instance, in the case of small correlation times compared to the membrane time constant, the response properties to periodic signals feature interesting effects [14,22]. Attempts to calculate the neural output statistics in the case of large correlation times have been

made by Moreno-Bote and Parga [20,23]. Considering synaptic filtering in the limit of large synaptic time constants, they use the quasideterministic membrane dynamics to derive expressions for the mean firing rate and the CV in the form of an infinite series of integrals.

Here, we present an analytical description of the ISI density of the LIF neuron driven by exponentially correlated Gaussian noise. We consider the limit of infinite correlation time but finite variance and find analytic approximations of the ISI density. In this limit the shape of this ISI density reflects a burstlike spiking dynamics that was already observed in [7,20]. Furthermore, we approximate the Fano factor for different time windows and derive an expression for the CV. The theoretical findings are compared with extensive numerical simulations, which also reveal unexpected properties of the SCC.

II. MODEL

The dynamics of the membrane potential $V(t)$ in the LIF model is described by the equation

$$\tau_m \dot{V} = -V + RI_s(t). \tag{1}$$

Therein the synaptic input current $I_s(t)$ is integrated with a membrane time constant τ_m. The first term on the right-hand side corresponds to the leak current $-V/R$, where R denotes the membrane resistance. The spike times t_i are determined by the moments when the membrane potential reaches the threshold value V_{th}. Afterwards, the membrane potential is reset to the value $V_r < V_{th}$ and the process continues according to Eq. (1). The synaptic input current I_s is considered to be a stationary Gaussian random process with mean $\tilde{\mu}$ and exponential correlation function $\langle I_s(t)I_s(t')\rangle - \tilde{\mu}^2 = (\tilde{\sigma}^2/2\tau_s)\exp(-|t-t'|/\tau_s)$. This can be realized by the linear equation

$$\tau_s \dot{I}_s = -I_s + \tilde{\mu} + \tilde{\sigma}\xi(t) \tag{2}$$

with white Gaussian noise $\xi(t)$ that obeys $\langle \xi(t)\xi(t')\rangle = \delta(t-t')$.

In the following we measure time in units of the membrane time constant (i.e., $t/\tau_m \to t$) and use the dimensionless variables $x=(V-V_r)/(V_{th}-V_r)$ and $y=R(I_s-\tilde{\mu})/(V_{th}-V_r)$. Furthermore, we introduce the quantities $D=\tilde{\sigma}^2R^2/[2\tau_m(V_{th}-V_r)^2]$, $\mu=(R\tilde{\mu}-V_r)/(V_{th}-V_r)$, and $\tau=\tau_s/\tau_m$ and rewrite Eqs. (1) and (2) as follows:

$$\dot{x} = -x + \mu + y, \quad \tau\dot{y} = -y + \sqrt{2D}\xi(t). \tag{3}$$

The membrane potential $x(t)$ is driven by the mean input current μ and the exponentially correlated Gaussian noise $y(t)$ with variance $\sigma^2 = D/\tau$ [Ornstein-Uhlenbeck process (OUP)]:

$$\langle y(t')y(t'+t)\rangle = \sigma^2 \exp(-|t|/\tau). \tag{4}$$

Whenever $x(t)$ reaches the threshold at $x_{th}=1$, the membrane potential is reset to the value $x=0$. The equality $x(t_i)=x_{th}$ again defines the spike times t_i and the corresponding ISIs $T_i = t_i - t_{i-1}$.

In the following we parametrize the colored noise $y(t)$ by the correlation time τ and the variance σ^2 as in Eq. (4). It guarantees a nonvanishing noise effect in the large τ limit. Fixing the variance allows for an easy comparison of spike trains with different τ, but similar firing rates. In fact, the firing rates (and other statistics) are largely affected by the magnitude of the membrane potential fluctuations—a trivial effect that we want to exclude. Hence the variance of these fluctuations $\sigma_x^2 = \langle x^2\rangle - \mu^2$ should ideally be constant upon variation of τ. It is easily revealed that

$$\sigma_x^2 = \frac{D}{\tau+1} = \frac{\sigma^2\tau}{\tau+1} \tag{5}$$

for the stationary process without reset. Because we consider the case $\tau \gg 1$, it is clear that σ_x keeps virtually constant if we fix σ^2. This noise scaling has been frequently used in different contexts [24,25]. In contrast, using the noise intensity D instead of the variance $\sigma^2 = D/\tau$ would allow the transition to white noise in the limit $\tau \to 0$ but would imply a vanishing of the noise in the limit $\tau \to \infty$. A quasideterministic dynamics of the membrane potential would have been established in the case of large correlation times: In the superthreshold regime ($\mu > 1$) the spike train becomes almost periodic, whereas the firing rate of noise-induced spiking becomes extremely small in the subthreshold regime ($\mu < 1$), in accordance to Eq. (5).

Note that our scaling of the noise is different from most existing works on the effect of synaptic filtering, where the noise is parametrized with D. This is because previous studies mostly concerned about small synaptic time constants $\tau \ll 1$. In this case the variance of x in Eq. (5) varies only a little when fixing the noise intensity D. Otherwise, the use of σ^2 would result in rather large variations. But even in the work [20,23], where the case $\tau \gg 1$ is considered, a fixed noise intensity D is used. This might be reasonable in the biological context of synaptic filtering, where the noisy input is smoothed by the synaptic capacitance at the expense of the variance (an approach unifying both limits in nonlinear dynamics has been proposed in [26,27]).

III. INTERSPIKE INTERVAL DENSITY

A. Inter- and intraburst intervals

Numerical simulations of the Langevin equation (3) give an instructive insight into the effect of colored noise on the spiking statistics. Figure 1 shows a typical trajectory of the membrane potential $x(t)$ and the OUP $y(t)$ for extremely long correlated noise ($\tau = 1000$). In this case, it becomes apparent that the firing activity is characterized by spike bursts that are closely related to the OUP. The main features of the corresponding ISI density are illustrated in Fig. 2(a): Increasing the correlation time, the ISI density becomes more and more concentrated around the most probable ISI. At the same time the tail of the distribution becomes extremely long and is expressed by a power-law decay. All curves show the usual time lag at small ISI's due to the relative refractory period and, at the other end of the distribution, an exponential cutoff for intervals that are much larger than the correlation time.

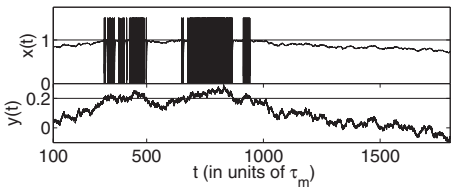

FIG. 1. Typical trajectories $x(t)$ and $y(t)$ in the case of extremely long correlated noise ($\tau=1000$). The upper panel depicts the dynamics of $x(t)$ below the threshold at $x=1$. [We note that the spikes above the threshold were not generated by the system Eq. (3), but have been added separately.] The corresponding evolution of the OUP $y(t)$ is shown in the lower panel. The level $b=1-\mu$ is indicated by the horizontal line. Other parameters are $\sigma^2=0.025$ and $\mu=0.8$.

The relative refractory period arises from the finite travel time of $x(t)$ from reset to threshold, which depends on the input current $\mu+y$. We also notice that the most probable ISI, indicating the maximum of the ISI density, stays practically unchanged for different τ.

The slow decay in the case of long correlated noise gives rise to extremely large but *infrequent* ISIs, which has noticeable implications on the common ISI statistics compared to *typical* properties of the ISIs. For instance, the *typical* ISI, which might be defined as $T_{typ}\sim\exp(\langle\ln T\rangle)$ (geometric mean), significantly differs from the mean ISI $\langle T\rangle$ [Fig. 2(b)]. The latter is virtually not altered for different correlation times, whereas the typical ISI decreases with τ until it saturates close to the most probable ISI. This is in accordance with the increasing skewness of the ISI density as depicted in Fig. 2(c). The skewness (or coefficient of asymmetry) is defined as $\gamma_a=k_3/k_2^{3/2}$ with the cumulants $k_2=\langle T^2\rangle-\langle T\rangle^2$ and $k_3=\langle T^3\rangle-3\langle T\rangle\langle T^2\rangle+2\langle T\rangle^3$. In addition to that, although more and more ISIs concentrate around the maximum of $f(T)$ and thus *typical* deviations become smaller for large correlation times, the standard deviation increases with τ. This is shown in Fig. 2(c) by the coefficient of variation (CV) $\gamma_v=(k_2/k_1^2)^{1/2}$ with $k_1=\langle T\rangle$. Apparently, the reason for the increase in variability for large correlation times is the presence of extreme ISIs. The impact of extreme but rare events on the variance of a random variable is usually expressed by its kurtosis (coefficient of excess). It is defined as $\gamma_e=k_4/k_2^2$, where in our case $k_4=\langle T^4\rangle-3\langle T^2\rangle^2-4\langle T\rangle\langle T^3\rangle+12\langle T\rangle^2\langle T^2\rangle-6\langle T\rangle^4$ is the fourth cumulant of the ISI density. Figure 2(c) reveals the rapid growth of the kurtosis (note the logarithmic scale), which is associated to the growing influence of extreme events on the neural variability.

The basic mechanism underlying this feature of the ISI density for long-correlated noise is quite simple. Due to a large correlation time τ the noise variable $y(t)$ is much slower than the membrane potential $x(t)$. Thus it happens that $y(t)$ is smaller than $1-\mu$ for a rather long time. However, if $y<1-\mu$ spiking is impossible since in this case $\dot{x}<0$ for all $x\leq 1$ so that the threshold cannot be reached with a non-negative velocity. Consequently, a period with $y(t)<1-\mu$ corresponds to a state without activity. We will refer to such a state as the *inactive state* of the neuron. As we

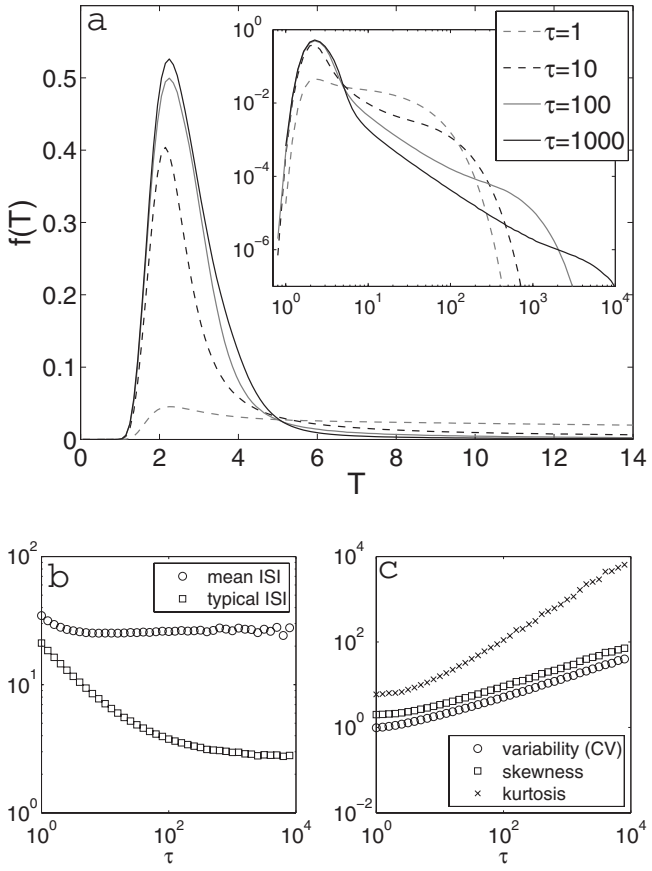

FIG. 2. (a) ISI densities for different indicated correlation times τ obtained from numerical simulations of the Langevin equation (3). With increasing τ the peak of the ISI density grows strongly as more probability accumulates around the most probable ISI (which keeps almost unaltered). The tails of the ISI densities are depicted in the double logarithmic plot (inset). Note the power law decay, which is most pronounced for $\tau=1000$, and the exponential cutoff at $T\sim\tau$. (b) Mean and typical ISI are plotted as a function of τ. Whereas the mean ISI is not altered by increasing τ, the typical ISI decreases monotonically toward an asymptotic value. (c) The variability (CV), skewness, and kurtosis of the ISI density as a function of τ. In all simulations $\mu=0.8$ and $\sigma^2=0.025$.

will see below, the durations of these inactive states follow a power law in the case of large correlation times. These durations can thus become very large and give rise to the extreme ISIs observed in simulations. In contrast, in periods where the slowly varying noise $y(t)$ is above $1-\mu$, the membrane potential $x(t)$ always reaches the threshold deterministically leading to fast and regular spiking. Thus the neuron operates virtually in a superthreshold regime. If $y(t)$ changes sufficiently slowly, these periods can contain numerous spikes resulting in a state of high activity. Thus we call the state with $y(t)>1-\mu$ the *active state*. The short, regular ISIs within the active state correspond to the high peak of the ISI density representing the small ISIs with its small variability. These ISIs are typical because one active state includes many ISIs, whereas the inactive state contributes only one ISI.

Because of the succession of active and inactive states the global structure strongly resembles neuronal *bursting*. Hence the overall process can be reduced to the switchings between

the two states, on the one hand, and the spiking structure within the active state, on the other hand. Since the active part shows a relatively regular spiking pattern, the large variability of the ISIs results from the random switching between states. This is in agreement with the conjecture that the variance strongly depends on the large ISIs, which are found among the interburst intervals (durations of the inactive states). The statistics of these switchings is solely determined by the OUP $y(t)$ relative to the level $b=1-\mu$.

This intuitive picture is now used to calculate the ISI density in the case of large correlation times τ. At first, we will analyze the distribution of ISIs within the active state (intraburst intervals), after which we will address the level crossings problem of $y(t)$. The latter yields the distribution of the interburst intervals (durations of the inactive states).

B. Distribution of intraburst intervals

In general, the ISI density can be written as an average of first-passage-time densities:

$$f(T) = \int f_{fp}(T|y)g(y)dy. \tag{6}$$

Here, $f_{fp}(T|y)$ is the first-passage-time density of the time T to reach the threshold at $x=1$ for the first time starting at $x=0$ with an initial value y. The average is computed over the probability density $g(y)$ of noise values $y(t_i)$ sampled at the moments of reset.

Generally the function $f_{fp}(T|y)$ is hard to calculate. However, in the limit $\tau\to\infty$ one can use the *quasistatic approximation* [16,20,23]. It means that on the time scale of short ISIs one assumes a frozen noise value $y=$const. Then according to $\dot{x}=-x+\mu+y$ the time from reset to threshold is given by

$$t^*(y) = \ln\left(\frac{y+\mu}{y+\mu-1}\right). \tag{7}$$

The first-passage-time density with given initial value y then yields

$$f_{fp}(T|y) = \delta[T - t^*(y)]. \tag{8}$$

Thus the quasistatic approximation is essentially a deterministic description of the ISIs and the only randomness originates from the distribution of the initial values of y.

In order to find the probability density $g(y)$ we consider the Fokker-Planck equation of the stationary probability density $p(x,y)$. It reads

$$[\partial_x(x-\mu-y) + \epsilon\partial_y(y+\sigma^2\partial_y)]p(x,y) = -J(y)\delta(x) \tag{9}$$

with the small parameter $\epsilon=1/\tau$ and the probability current through the threshold $J(y)=(-x+\mu+y)p(x,y)|_{x=1}$ at a given value y. Equation (9) is supplemented by the following conditions:

$$p(1,y) = 0, \quad \forall\ y < b, \tag{10}$$

$$\lim_{y\to\pm\infty} p(x,y) = \lim_{y\to\pm\infty} \frac{\partial p}{\partial y} = \lim_{x\to-\infty} p(x,y) = 0, \tag{11}$$

$$\int_{-\infty}^{\infty}\int_{-\infty}^{1} p(x,y)dxdy = 1. \tag{12}$$

The condition (10) prevents trajectories from recrossing the threshold with a negative velocity. Equations (11) and (12) represent the obvious boundary conditions at infinity and the normalization condition. The reset mechanism is accomplished by the source term on the right-hand side of Eq. (9): The probability current $J(y)$ which flows at y across the threshold is reinserted at $x=0$ with the same value of y. Thus, the probability density $g(y)$ of finding y upon resetting must be proportional to $J(y)$.

In the following, the goal will be to calculate $J(y)$ in lowest order of ϵ corresponding to the limit $\tau\to\infty$. Assuming that $p(x,y)$ and $J(y)$ can be expanded in orders of ϵ with leading terms $p_0(x,y)$ and $J_0(y)$, Eq. (9) becomes in zeroth-order

$$\partial_x(x-\mu-y)p_0(x,y) = -J_0(y)\delta(x). \tag{13}$$

Note that in accordance to the quasistatic approximation, the drift and diffusion in the y direction plays no role anymore. Integrating over x gives

$$p_0(x,y) = \frac{J_0(y)}{y+\mu-x}\theta(x),$$

where $\theta(x)$ is the Heaviside function. Further integrating yields

$$\int_{-\infty}^{1} p_0(x,y)dx = J_0(y)\int_0^1 \frac{dx}{y+\mu-x},$$

from which $J_0(y)$ can be obtained. In fact, the left-hand side of the last relation gives the marginal distribution of y, which is

$$P(y) = \frac{1}{\sqrt{2\pi}\sigma}\exp\left(-\frac{y^2}{2\sigma^2}\right), \tag{14}$$

and the integral on the right-hand side yields $t^*(y)$. Thus we obtain

$$g_0(y) \propto J_0(y) = \frac{P(y)}{t^*(y)}\theta(y-b). \tag{15}$$

We found from simulations that the expression of the quasistatic approximation fits very well the density of y values at the threshold except for values close to the sharp peak near $y=b$ [Fig. 3(a) and 3(b)]. The reason for that is due to the quasistatic approximation, where we so far analyzed only the ISIs within the active state, not taking into account the interburst intervals. The sharp peak of $g(y)$ at $y\approx b$ arises from initial conditions of those trajectories $y(t)$ that become smaller than b before the next firing time. Hence these trajectories induce a new inactive state. Consequently, the peak corresponds to the initial conditions of starting an inactive state. Oppositely, the part of $g(y)$ without peak reflects indeed the initial noise values within the active state.

According to Eqs. (6) and (8) and using the properties of the δ function we find

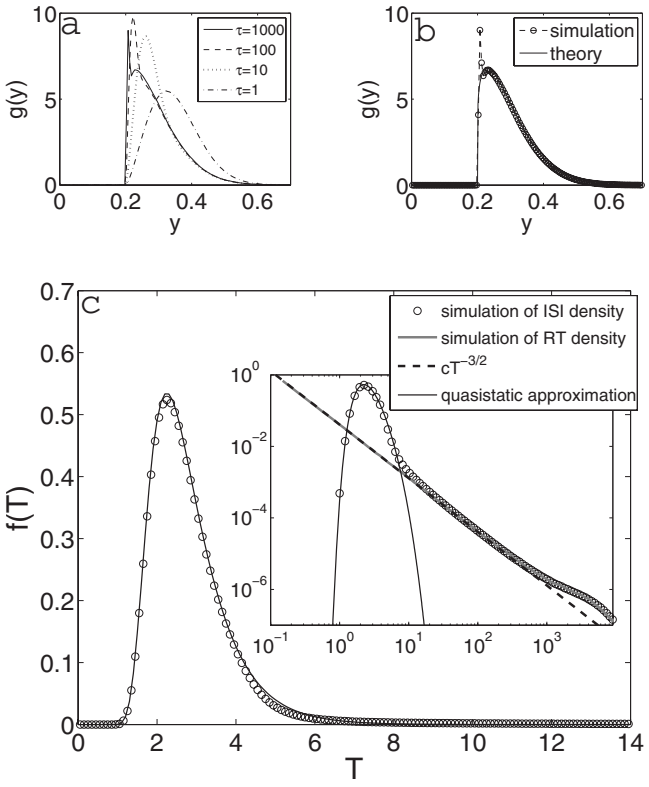

FIG. 3. (a) Simulated noise-upon-firing density $g(y)$ for different indicated correlation times τ. (b) Quasistatic approximation of $g(y)$ compared to the simulation result for $\tau=1000$. (c) ISI density in the quasistatic approximation compared to the simulated ISI density for $\tau=1000$. Inset of (c): The double logarithmic plot shows that the quasistatic approximation does not apply to intermediate and long ISIs. They can be recovered by the recurrence time (RT) density of the OUP as revealed from simulations of the level crossings of the OUP. The theoretically predicted power law $f(T)=cT^{-3/2}$ for $T \ll \tau$ can be well fitted to the intermediate ISIs and to the simulated RT density ($\sigma^2=0.025$, $\mu=0.8$).

$$f_0(T) = \int_b^\infty \delta\left(T - \ln\left(\frac{y+\mu}{y+\mu-1}\right)\right) g_0(y)dy$$
$$= \varphi(T)[\varphi(T)-1]g_0(\varphi(T)-\mu),$$

with

$$\varphi(T) = \frac{1}{1-e^{-T}}. \tag{16}$$

Using Eq. (15) the ISI density in the quasistatic approximation yields (except for a normalization factor)

$$f_0(T) \propto \frac{1}{T(\cosh T - 1)} \exp\left(-\frac{(\varphi(T)-\mu)^2}{2\sigma^2}\right). \tag{17}$$

This expression constitutes the limit of infinitely large correlation time τ. Figure 3(c) shows that for small ISIs belonging to the active state this limit is in good agreement with the ISI density for the large but finite correlation time $\tau=1000$. The time scale of these intraburst intervals is much smaller than the relaxation time τ of the OUP. Thus the quasistatic approximation is valid since $y(t)$ can be assumed constant. Figure 2(a) suggests also that in the case $\tau=100$ this expression describes the ISI density for intraburst intervals reasonably well. The good agreement, however, breaks down for correlation times that are not much larger than the intraburst intervals, which are of the order $T \sim 2$. In this case the quasistatic approximation is not suitable, which becomes clear in Fig. 2(a): the ISI density for $\tau=10$ already significantly deviates from the case $\tau=1000$.

The quasistatic approximation cannot reproduce the correct distribution of the intermediate and long ISIs as can be seen in the inset of Fig. 3(c). This is clear, because the quasistatic theory does not account for the noise-induced interburst intervals.

C. Durations of the inactive states

In order to describe the distribution of the interburst intervals we address the duration of the inactive state, i.e., the period of time in which $y(t)$ stays below the level $b=1-\mu$. To see that in the case of large τ this duration equals an interburst interval, we note that without resetting the fast variable $x(t)$ adiabatically adjusts to the slowly varying variable $\bar{x}(t)=y(t)+\mu$ [24]. This is because averaging over the fast motion of $x(t)$ implies $\dot{\bar{x}}=0$. Hence on typical time scales of y a level crossing of $y(t)$ with respect to the level $b=1-\mu$ entails also a threshold crossing of the membrane potential $\bar{x}(t)$ at $x=1$. In particular, any active state between two adjacent inactive states must include at least one spike.

By definition, an inactive state is given by the time interval between a crossing of $y(t)$ of the level b from above and the successive recurrence of $y(t)$ to the level b from below. Let us further consider a finite time interval that is sufficiently large; in particular the length of the interval δt should be much larger than the durations of inactive states under consideration. If we denote, with respect to this interval, the mean number of inactive states whose duration exceeds a given minimum duration T by $\nu(T)\delta t$, the associated recurrence time "density" can be expressed by

$$\Phi(T) = -\frac{d\nu}{dT}. \tag{18}$$

However, $\Phi(T)$ cannot be normalized to yield a probability density function, since $y(t)$ is a continuous Markov process. In fact, there exist infinitely many level crossings in any neighborhood of a given level crossing due to the unbound derivative $dy(t)/dt$, which permanently changes sign. Consequently, $\nu(T)$ becomes infinitely large as T approaches zero and hence the integral $\int_0^\infty \Phi(T)dT$ diverges. Nevertheless, $\Phi(T)$ has still a well defined meaning: $\Phi(T)dT\delta t$ is the mean number of inactive states (in a large interval of length δt) with a duration in $[T, T+dT]$. Thus $\Phi(T)$ can be seen as the *unnormalized* recurrence time density.

It seems that there exists no explicit solution for $\nu(T)$ in the case of a general OUP with $b \neq 0$. However, if we confine ourselves to small or intermediate interburst intervals $T \ll \tau$, we can assume that $y(t)$ undershoots the level b only by a

small amount. Hence in this limit the restoring force $-y/\tau$ can be assumed constant in the vicinity of b. According to [28], we readily obtain in this approximation

$$\nu(T) = \frac{b}{2\tau} P(b) \left[\frac{-\vartheta}{\sqrt{\pi\vartheta}} - \mathrm{erfc}\,\sqrt{\vartheta} \right], \tag{19}$$

with

$$\vartheta = \frac{1}{4}\frac{b^2}{\sigma^2}\frac{T}{\tau}$$

and $P(b)=\exp(-b^2/2\sigma^2)/\sqrt{2\pi\sigma^2}$. Differentiating $\nu(T)$ the unnormalized recurrence time density for the case that $y(t)$ falls below the level b only a little yields

$$\Phi(T) = \frac{1}{\pi\sigma^2}\left(\frac{T}{2\tau}\right)^{-3/2} \exp\left[-\frac{b^2}{2\sigma^2}\left(\frac{T}{2\tau}+1\right)\right]. \tag{20}$$

The asymptotical decay of Eq. (20) for $T \ll \tau$ is $\Phi(T) \propto T^{-3/2}$ confirming our observation of a power law for large correlation times. Indeed, the power law with exponent $-3/2$ well fits the intermediate tail of the ISI density as can be seen in the inset of Fig. 3(c).

IV. OTHER MEASURES OF NEURAL RESPONSE

Due to the presence of temporal correlations the point process naturally becomes nonrenewal. Therefore the question arises whether the ISI density is sufficient or if other, higher-order measures must be taken into account to describe the effect of long-correlated noise. To this end, two possible statistical descriptions of nonrenewal processes are often utilized. First, one might consider the statistics of the spike count $N(t)$ in a fixed time window of length t for all lengths $t>0$. As a matter of fact, the statistics of the count process $N(t)$ contains the full information about the nonrenewal point process. A commonly used measure of the variability of this count process is the Fano factor defined as

$$F(t) = \frac{\langle N(t)^2\rangle - \langle N(t)\rangle^2}{\langle N(t)\rangle}, \tag{21}$$

which is the variance-to-mean ratio of $N(t)$. It expresses the variability of the spike train on a certain time scale t. Moreover, it allows for a simple comparison with a Poisson process, for which the Fano factor equals 1 on every time scale. Second, one might also consider the correlations within the ISI sequence $\{T_1, T_2, T_3, \ldots\}$ in order to characterize the nonrenewal process. For several systems that generate point processes it has been found that the effect of long-correlated noise appears in the interval correlations rather than in the single interval statistics. Examples include the PIF neuron model discussed in the Introduction and, as recently shown, residence time sequences of bistable systems [29].

A. The Fano factor

To compute the Fano factor analytically in the case of large correlation time τ, we replace the actual spike train by a modified process. Specifically, we assume that within the active state spikes occur independently at times t_i with constant rate r. This rate might be approximated by the inverse most probable ISI. We recall that r is virtually independent of τ. Doing so, we aim only at the description of the count process on time scales that are much larger than $1/r$ neglecting the short-time structure of the count process. Introducing the spike train $n(t)=\Sigma_i \delta(t-t_i)$ and the indicator function of the active state $s(t)=\theta[y(t)-b]$, where $\theta(x)$ denotes again the Heaviside function, we can express the counting process as

$$N(t) = \int_0^t n(t')s(t')dt'. \tag{22}$$

Because of the stationarity of $y(t)$ and the independence of $n(t)$ and $s(t)$ we easily find the mean of $N(t)$,

$$\langle N(t)\rangle = \langle s\rangle rt \tag{23}$$

with

$$\langle s\rangle = \int_b^\infty \frac{dy}{\sqrt{2\pi}\sigma}\exp\left(-\frac{y^2}{2\sigma^2}\right) = \frac{1}{2}\mathrm{erfc}\left(\frac{b}{\sqrt{2}\sigma}\right). \tag{24}$$

This result also confirms our conjecture that the mean firing rate $\langle N(t)\rangle/t=\langle s\rangle r$ and consequently the mean ISIs

$$\langle T\rangle = \frac{1}{\langle s\rangle r} \tag{25}$$

are independent of the correlation time τ [Fig. 2(b)]. The variance $\langle \Delta N(t)^2\rangle = \langle N(t)^2\rangle - \langle N(t)\rangle^2$ can be calculated as follows:

$$\begin{aligned}\langle \Delta N(t)^2\rangle &= \int_0^t\int_0^t \langle n(t_1)n(t_2)\rangle\langle s(t_1)s(t_2)\rangle dt_1 dt_2 - \langle s\rangle^2 r^2 t^2 \\ &= r^2\int_0^t\int_0^t C(t_1-t_2)dt_1dt_2\end{aligned} \tag{26}$$

with the correlation function

$$C(t) = \langle s(0)s(t)\rangle - \langle s\rangle^2. \tag{27}$$

This correlation function is known for the limits of small times $t \ll \tau$ and large times $t \gg \tau$ [30]. In particular, the correlation function for small times $C_s(t)$ is given by

$$C_s(t) = C(0) - \frac{A}{\pi\sqrt{2}}\left(\frac{t}{\tau}\right)^{1/2}, \tag{28}$$

where $C(0)=\langle s\rangle(1-\langle s\rangle)$ and $A=\exp[-b^2/(2\sigma^2)]$. From this we obtain the Fano factor in the small-time limit as

$$F(t) = (1-\langle s\rangle)rt - \frac{4A}{15\pi}\sqrt{\frac{2}{\tau}}\frac{r}{\langle s\rangle}t^{3/2}. \tag{29}$$

Since the first term dominates for small t, the Fano factor grows approximately linearly.

For large times $t \gg \tau$ the correlation function $C_l(t)$ can be approximated as [30]

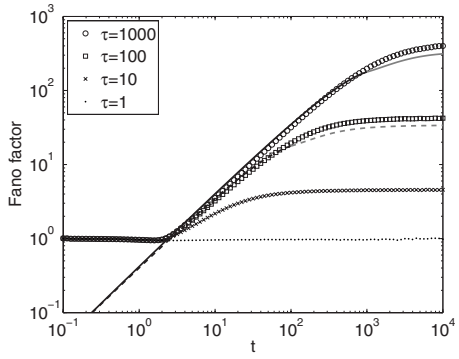

FIG. 4. Fano factor as a function of the time window length t for different correlation times as indicated. Symbols denote simulation results, whereas the solid (dashed) line shows the theoretical result for $\tau=1000$ ($\tau=100$). The black part of the theoretical curves ($t<\tau$) is given by Eq. (29) and the gray part ($t\geq\tau$) corresponds to Eq. (31). The free prefactor r describing the firing rate within the active state was chosen as $r=(2.1)^{-1}$ ($\sigma^2=0.025$, $\mu=0.8$).

$$C_l(t)=\frac{A^2}{2\pi}\exp(-t/\tau). \tag{30}$$

According to Eq. (26) the calculation of the Fano factor for large time windows t involves the integration of $C(t)$ over the whole interval $[0,t]$, which actually requires the knowledge of $C(t)$ for intermediate times as well. An explicit expression for $C(t)$ for intermediate times is, however, hard to obtain. In order to derive an estimation of $F(t)$, we assume that $C(t)\approx C_s(t)$ for $t\leq\tau$ and $C(t)\approx C_l(t)$ for $t>\tau$. Because of the symmetry $C(-t)=C(t)$ of the correlation function, we further transform the double integral of Eq. (26) into a single integral:

$$\int_0^t\int_0^t C(t_1-t_2)dt_1dt_2=2\int_0^t(t-t')C(t')dt'.$$

Using this relation, the Fano factor for times $t>\tau$ yields

$$F(t)=F_\infty-\frac{r\tau^2}{t}\left[1-\langle s\rangle-\frac{A^2}{\pi\langle s\rangle}\left(e^{-t/\tau}+\frac{2\sqrt{2}}{5A}-\frac{2}{e}\right)\right] \tag{31}$$

with

$$F_\infty=r\tau\left[2(1-\langle s\rangle)+\frac{A}{\pi\langle s\rangle}\left(\frac{A}{e}-\frac{2\sqrt{2}}{3}\right)\right]. \tag{32}$$

Apparently, for infinitely large time windows ($t\to\infty$) the Fano factor saturates at the finite value F_∞. Figure 4 shows that our estimation agrees well with results of numerical simulation of the Fano factor for moderate and long time windows. By construction of the modified spike train it is clear that our result cannot explain the short-time behavior of the counting statistics of the actual spike pattern. The simulation results reveal, however, that we do not expect a deep minimum at a certain time scale in the LIF model, in contrast to the observations made for the PIF neuron model [15–17].

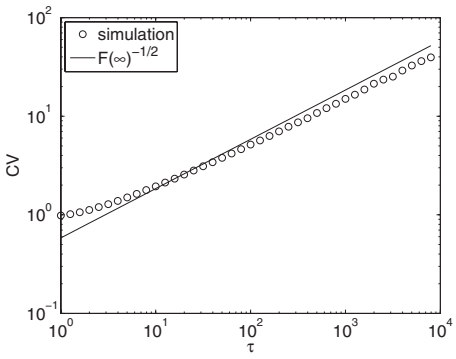

FIG. 5. CV as a function of the correlation time τ. Symbols depict the simulation result and the solid line shows $\sqrt{F_\infty}\propto\sqrt{\tau}$. As in Fig. 4, we choose the prefactor r as $r=(2.1)^{-1}$ ($\sigma^2=0.025$, $\mu=0.8$).

The large-time behavior F_∞ gives an interesting link between the count statistics and the interval statistics. Indeed, for a renewal point process the Fano factor is linked with the coefficient of variation γ_v by $F_\infty=\gamma_v^2$ [31]. In general, this relation does not apply to nonrenewal processes. But, as suggested in [20], this can still give a reasonable approximation of the CV. In particular, from Eq. (32) we find that the CV rises like the square root of the correlation time:

$$\gamma_v\approx\sqrt{F_\infty}\propto\sqrt{\tau}. \tag{33}$$

This behavior is indeed confirmed by simulations: Figure 5 shows a good agreement of our approximation. It suggests that despite the long correlations inherent in the driving, the resulting spike train might be treated as a renewal process.

B. The serial correlation coefficient

To support the last conjecture we calculated the serial correlation coefficient (SCC), which we obtained from simulations. The SCC is a common measure to characterize correlations between ISIs. It is defined as the covariance of ISIs that are lagged by an integer n normalized by the variance of the ISIs:

$$\rho_n=\frac{\langle T_kT_{k+n}\rangle-\langle T_k\rangle\langle T_{k+n}\rangle}{\langle T_k^2\rangle-\langle T_k\rangle^2}. \tag{34}$$

Therein, ρ_n denotes the nth SCC and the averages are performed over the index k.

Before discussing the SCC for the LIF model, it is useful to recall the corresponding results for the simpler PIF neuron model driven by the OUP, which was previously studied in [16]. There it has been found that the SCC as a function of the lag n obeys a simple exponential law: $\rho_n^{\mathrm{PIF}}=\exp(-n\langle T\rangle/\tau)$. This is a remarkable result, because it allows us to directly determine an underlying correlation time τ from a measurement of the SCC and the mean ISI. The SCC for the PIF model is illustrated in Fig. 6. It reveals that the magnitude of the SCC is close to 1 for sufficiently small lags (depending on τ) expressing strong ISI correlations. Furthermore, in the PIF model an increasing correlation time results in a larger SCC.

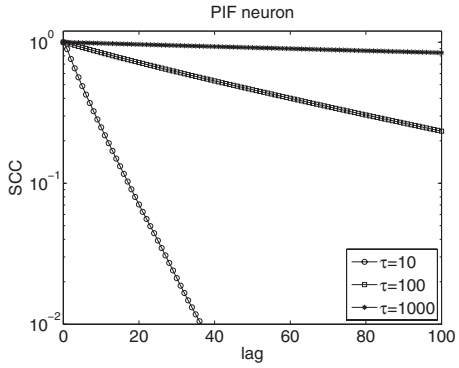

FIG. 6. The SCC for the PIF neuron model as a function of the lag (adopted from [16]). In comparison to the LIF model, the PIF model lacks a "restoring force" (leakage) and reads $\dot{x}=\mu+y$. The parameters are $\mu=0.8$ and $\sigma^2=0.025$.

The LIF model only differs from the PIF model by the introduction of a leak current. Figure 7 shows, however, that the SCC for the LIF model has a very different behavior: the SCC in the subthreshold case ($\mu<1$) as well as in the superthreshold case ($\mu>1$) are comparatively small. Moreover, we do not recover the property that larger correlation times generate larger SCCs as it can be seen in Fig. 7(b), where on the contrary ρ_1 decreases with increasing τ. The decreasing behavior of ρ_1 for large correlation times is indeed confirmed by simulations: Figure 8 suggests that the SCC vanishes in

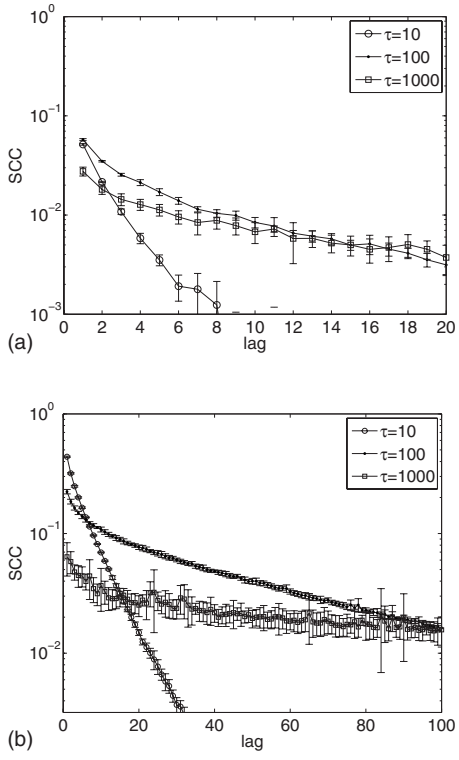

FIG. 7. Serial correlation coefficient as a function of the lag for different correlation times as indicated ($\sigma^2=0.025$). (a) Subthreshold case $\mu=0.8$, (b) superthreshold case $\mu=1.3$. Note the different scalings of the axes.

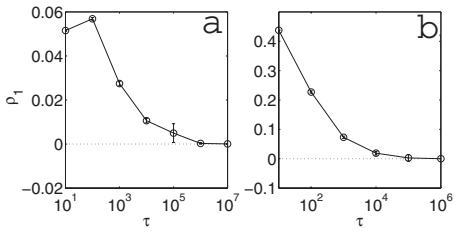

FIG. 8. Symbols show ρ_1 as a function of the correlation time τ. Like in Fig. 7, the left panel (a) depicts the subthreshold case $\mu=0.8$, whereas the right panel (b) depicts the superthreshold case $\mu=1.3$. The data were obtained from simulation of the Langevin equation (3).

the limit $\tau\to\infty$. Assuming that correlations decay with increasing lag, this would imply that also higher-order SCCs vanish, i.e., for all $n\geq 1$ it holds that

$$\lim_{\tau\to\infty}\rho_n=0. \tag{35}$$

The vanishing of ρ_1 for infinitely large correlation times can be intuitively understood. First, we note that the variance of ISIs grows *linearly* in τ as shown in the previous section. In fact, according to Eq. (33) the variance is proportional to $\tau\langle T\rangle^2$ and the mean ISI $\langle T\rangle$ is constant with respect to τ. We recall that the latter is a result of the noise scaling we used, which ensures a constant firing rate for large τ (cf. Sec. II). Second, in order to prove that ρ_1 vanishes in the limit of large correlation times, we show that the covariance $\langle T_kT_{k+1}\rangle-\langle T\rangle^2$ is asymptotic to a constant in this limit. To this end, we proceed similarly as in the previous section: we consider a slightly modified spike train, where the intraburst intervals are replaced by intervals of length equal to the mean intraburst interval $1/r$. As stated before, the mean intraburst interval $1/r$ is not affected by large correlation times and can be treated as constant. From these assumptions we find that $\langle T_kT_{k+1}\rangle-\langle T\rangle^2=1/r\langle T\rangle-\langle T\rangle^2=\text{const}$, since either T_k or T_{k+1} must be an intraburst interval (two interburst intervals are separated by at least one intraburst interval). Thus we conclude that the SCC indeed approaches zero in the large τ limit due to a diverging variance.

Note that although the absolute values of the SCCs become smaller for larger correlation times, the decay with respect to the lag gets slower for larger τ. This can be seen in Fig. 7 and reveals that large correlation times induce long-range correlations in the ISI sequence.

V. CONCLUSIONS

We analyzed the ISI density of a LIF neuron driven by long-correlated Gaussian noise and described its implications on the firing statistics. In particular, the large skewness and kurtosis of the ISI density indicates the influence of extremely large ISIs, which is expressed by a diverging CV and a suppressed serial correlation coefficient. Moreover, the shape of the ISI density completely reflects the bursting behavior in the case of large correlation times. This is revealed by a pronounced peak corresponding to intraburst intervals, and a power-law tail that corresponds to interburst intervals.

Thus typical neural firing properties like high variability and bursting can be simply generated by using colored noise with a large correlation time. The fact that a slow subsystem controls the fast neuron dynamics yields indeed a quite common and intuitive mechanism for bursting [32–34]. Recently, it was also shown by information-theoretic measures that low frequency signals can be encoded by bursts in spike trains of pyramidal neurons [35]. It is interesting that in that paper the experimental data could be modeled also using a LIF model. However, the bursting pattern was achieved in a rather different way by including an explicit depolarizing spike-response current. The latter accounted for a depolarizing afterpotential that followed each action potential. It would be interesting whether this combination of LIF model and spike-response model could be approximately mapped to the simpler, stationary process investigated in the present work.

By analyzing active and inactive states separately, we derived an analytical expression for the density of intraburst intervals in the limit $\tau \to \infty$ and explained the power-law exponent of $-3/2$ for the interburst intervals. The derivation of the intraburst interval distribution relied on a time scale separation technique similar as in [16,20,23]. For the PIF neuron model considered in [16], the quasistatic approximation for the ISI density holds down to correlation times of order $\tau \sim 10$. Thus the region of applicability of this approximation shrinks in the more realistic LIF model, for which the method could well reproduce ISI densities down to $\tau \sim 100$. This is due to stronger variations of the deterministic travel time $t^*(y)$ in the LIF model in the case when y cannot be assumed static anymore (note that this time even diverges if $y \to 1-\mu$).

The picture of active and inactive states in the case of large correlation times also allowed us to analytically calculate the Fano factor of the LIF neuron. From this we could obtain an expression for the CV other than infinite series formulas previously found for the LIF neuron driven by dichotomous colored noise [15] and Ornstein-Uhlenbeck noise [20]. In this paper we explained the asymptotic behavior of the CV for large correlation times, which diverges like $\sqrt{\tau}$.

As a consequence of the diverging behavior of the CV we were able to prove a surprising observation: The serial correlation coefficient of the LIF neuron approaches zero in the limit of infinitely large correlation times. This result is qualitatively different from the effect of colored noise in the PIF neuron [15–17]. It means that due to the introduction of a leak current, the spike train can be effectively treated as a renewal process in the large τ limit.

ACKNOWLEDGMENTS

L.S.G. thanks Sfb555 of the Deutsche Forschungsgemeinschaft and Bernstein-Center for Computational Neuroscience Berlin for support. T.S. thanks the German National Academic Foundation for support.

[1] G. Gerstein and B. Mandelbrot, Biophys. J. **4**, 41 (1964).
[2] R. B. Stein, Biophys. J. **5**, 173 (1965).
[3] L. M. Ricciardi and L. Sacerdote, Cybernetics **35**, 1 (1979).
[4] P. Lansky, J. Theor. Biol. **107**, 631 (1984).
[5] P. Lansky and V. Lanska, Biol. Cybern. **56**, 19 (1987).
[6] A. N. Burkitt, Biol. Cybern. **95**, 1 (2006).
[7] G. Svirskis and J. Rinzel, Biophys. J. **79**, 629 (2000).
[8] A. Longtin, J. Stat. Phys. **70**, 309 (1993).
[9] A. Longtin, A. Bulsara, and F. Moss, Phys. Rev. Lett. **67**, 656 (1991).
[10] A. R. Bulsara, T. C. Elston, C. R. Doering, S. B. Lowen, and K. Lindenberg, Phys. Rev. E **53**, 3958 (1996).
[11] H. E. Plesser and T. Geisel, Phys. Rev. E **59**, 7008 (1999).
[12] B. Lindner and L. Schimansky-Geier, Phys. Rev. Lett. **86**, 2934 (2001).
[13] M. Schindler, P. Talkner, and P. Hänggi, Phys. Rev. Lett. **93**, 048102 (2004).
[14] N. Fourcaud and N. Brunel, Neural Comput. **14**, 2057 (2002).
[15] E. Salinas and T. J. Sejnowski, Neural Comput. **14**, 2111 (2002).
[16] J. W. Middleton, M. J. Chacron, B. Lindner, and A. Longtin, Phys. Rev. E **68**, 021920 (2003).
[17] B. Lindner, Phys. Rev. E **69**, 022901 (2004).
[18] L. Lapicque, J. Physiol. Pathol. Gen. **9**, 620 (1907).
[19] N. Brunel and S. Sergi, J. Theor. Biol. **195**, 87 (1998).
[20] R. Moreno-Bote and N. Parga, Phys. Rev. Lett. **96**, 028101 (2006).
[21] T. Verechtchaguina, I. M. Sokolov, and L. Schimansky-Geier, Phys. Rev. E **73**, 031108 (2006).
[22] N. Brunel, F. S. Chance, N. Fourcaud, and L. F. Abbott, Phys. Rev. Lett. **86**, 2186 (2001).
[23] R. Moreno-Bote and N. Parga, Phys. Rev. Lett. **92**, 028102 (2004).
[24] W. Horsthemke and R. Lefever, *Noise Induced Transitions* (Springer, Berlin, 1984).
[25] I. Sendiña-Nadal, S. Alonso, V. Pérez-Muñuzuri, M. Gómez-Gesteira, V. Pérez-Villar, L. Ramírez-Piscina, J. Casademunt, J. M. Sancho, and F. Sagués, Phys. Rev. Lett. **84**, 2734 (2000).
[26] P. Jung and P. Hänggi, Phys. Rev. A **35**, 4464 (1987).
[27] P. Hänggi and P. Jung, Adv. Chem. Phys. **89**, 239 (1995).
[28] R. L. Stratonovich, *Topics in the Theory of Random Noise* (Gordon and Breach, New York, 1967), Vol. 2.
[29] B. Lindner and T. Schwalger, Phys. Rev. Lett. **98**, 210603 (2007).
[30] P. Jung, Phys. Rev. E **50**, 2513 (1994).
[31] D. R. Cox, *Renewal Theory* (Methuen, London, 1962).
[32] E. M. Izhikevich, *Dynamical Systems in Neuroscience: The Geometry of Excitability and Bursting* (MIT Press, Cambridge, MA, 2005).
[33] A. B. Neiman and D. F. Russell, Phys. Rev. Lett. **88**, 138103 (2002).
[34] S. Liepelt, J. A. Freund, L. Schimansky-Geier, A. Neiman, and D. F. Russell, J. Theor. Biol. **237**, 30 (2005).
[35] A. M. O. B. Doiron and L. Maler, J. Neurophysiol. **97**, 2744 (2007).